Research Paper

ADvanced IMage Algebra (ADIMA): a novel method for depicting multiple sclerosis lesion heterogeneity, as demonstrated by quantitative MRI

Marios C Yiannakas[1], Daniel J Tozer[1], Klaus Schmierer[1,2,3], Declan T Chard[1], Valerie M Anderson[1], Daniel R Altmann[1,4], David H Miller[1] and Claudia AM Wheeler-Kingshott[1]

Abstract

Background: There are modest correlations between multiple sclerosis (MS) disability and white matter lesion (WML) volumes, as measured by T2-weighted (T2w) magnetic resonance imaging (MRI) scans (T2-WML). This may partly reflect pathological heterogeneity in WMLs, which is not apparent on T2w scans.

Objective: To determine if ADvanced IMage Algebra (ADIMA), a novel MRI post-processing method, can reveal WML heterogeneity from proton-density weighted (PDw) and T2w images.

Methods: We obtained conventional PDw and T2w images from 10 patients with relapsing–remitting MS (RRMS) and ADIMA images were calculated from these. We classified all WML into bright (ADIMA-b) and dark (ADIMA-d) sub-regions, which were segmented. We obtained conventional T2-WML and T1-WML volumes for comparison, as well as the following quantitative magnetic resonance parameters: magnetisation transfer ratio (MTR), T1 and T2. Also, we assessed the reproducibility of the segmentation for ADIMA-b, ADIMA-d and T2-WML.

Results: Our study's ADIMA-derived volumes correlated with conventional lesion volumes ($p < 0.05$). ADIMA-b exhibited higher T1 and T2, and lower MTR than the T2-WML ($p < 0.001$). Despite the similarity in T1 values between ADIMA-b and T1-WML, these regions were only partly overlapping with each other. ADIMA-d exhibited quantitative characteristics similar to T2-WML; however, they were only partly overlapping. Mean intra- and inter-observer coefficients of variation for ADIMA-b, ADIMA-d and T2-WML volumes were all < 6 % and < 10 %, respectively.

Conclusion: ADIMA enabled the simple classification of WML into two groups having different quantitative magnetic resonance properties, which can be reproducibly distinguished.

Introduction

Multiple sclerosis (MS) is a chronic inflammatory disease of the central nervous system (CNS), characterised by the presence of demyelinating white matter lesions (WML). WML can be detected using magnetic resonance imaging (MRI): They are seen as areas of high signal intensity on proton density-weighted (PDw) and T2-weighted (T2w) magnetic resonance (MR) images (T2-WML). However, studies show that the volume of T2-WML correlates only modestly with clinical disability, a phenomenon referred

[1]University College London (UCL), Institute of Neurology, London, UK.
[2]Blizard Institute, Centre for Neuroscience and Trauma, London, UK.
[3]Barts and The London School of Medicine and Dentistry, London, UK.
[4]London School of Hygiene and Tropical Medicine, London, UK.

Corresponding author:
Marios C Yiannakas, Department of Neuroinflammation, University College London (UCL), Institute of Neurology, Queen Square House, Queen Square, London, WC1N 3BG, UK.
Email: m.yiannakas@ucl.ac.uk

to as a clinico-radiologic paradox.[1] The observed dissociation has been attributed, in part, to the inability of PDw and T2w MRI to identify the underlying pathologic heterogeneity of T2-WML, but also to factors other than T2-WML.

Whilst a plethora of in vivo MR studies aim to characterise the underlying pathological processes that exist beyond T2-WML, i.e. in normal-appearing white matter (NAWM)[2–7] and dirty-appearing white matter (DAWM),[8–11] in an effort to explain the observed clinico-radiological dissociation pertaining to T2-WML volume measurements, very little work probes the pathological tissue heterogeneity that exists within and between WML that are seen on routine PDw and T2w images. The possible contribution of such findings toward resolving the clinico-radiologic dissociation currently remains unknown.

ADvanced IMage Algebra (ADIMA) is a novel MR image-processing method that utilises conventional PDw and T2w data-sets to classify all WML on these images into either 'bright' or 'dark' ADIMA sub-regions, which can be easily segmented, reflecting underlying tissue heterogeneities that have not been previously investigated. In this publication, the ADIMA method is described along with the results from preliminary investigations to (a) assess the reproducibility of segmenting the ADIMA-derived regions, (b) determine any correlations between the ADIMA-derived volumes and conventional lesion volumes, i.e. T2-WML and T1-WML and (c) characterise the properties of the underlying tissue within these ADIMA-derived regions, by means of quantitative MRI, i.e. T1, T2 and magnetisation transfer ratio (MTR).

Materials and methods

The ADIMA method

The technique of 'pseudo-T1' image contrast is reported in the literature.[12] Typically, a pseudo-T1 image is obtained through a pixel-by-pixel subtraction of the late echo image seen in a conventional fast-spin echo (FSE) dual-echo (T2w) data-set from the corresponding early echo (PDw), yielding an image that appears qualitatively similar to a conventional T1-weighted image (T1w), that is, the cerebrospinal fluid (CSF) and lesions having long T2 relaxation times appear hypointense, relative to NAWM (see Figure 1). The PDw and T2w images are acquired with a dual-echo sequence, which means they are co-registered and have the same transmitter and receiver gain settings. The pseudo-T1 image contains both negative and positive pixel values.

The ADIMA method's rationale is based on expanding the dynamic range of signal intensities in the final ADIMA image, in order to visualise subtle differences within tissue types. This is achieved by applying a normalisation operation to both the pseudo-T1 and the original PDw image
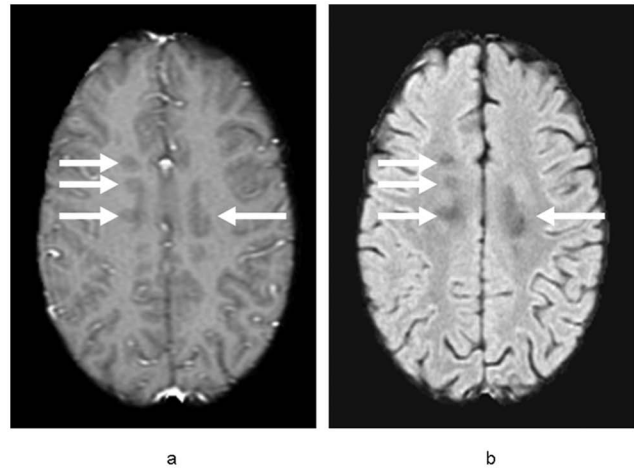

Figure 1. (a) T1w image in an MS patient and (b) the corresponding pseudo-T1 image produced from the subtraction of the late echo from the early echo, in a conventional FSE dual-echo data-set that was acquired in the same scanning session. White arrows indicate the presence of MS lesions.
FSE: fast-spin echo; MS: multiple sclerosis; T1: T1-weighted.

(referred to as *image* in equation (1)). If max_a = max (image) and min_a = min (image), then:

$$image\_normalised = (image - min\_a) / (max\_a - min\_a) \quad (1)$$

During the operation in equation (1), the images are normalised from the original 16-bit signed integer arrays of the PDw image and the pseudo-T1 image, into double-precision arrays with values in the range 0–1. Next, the absolute intensity difference between the two is calculated to obtain the ADIMA image as follows in equation (2):

$$ADIMA\_image = |PDimage\_normalised - pseudoT1\_normalised| \quad (2)$$

Without the normalisation step, equation (2) would lead to the original T2w image, but because of the operation described in equation (1), the image resulting from the subtraction described in equation (2) exhibits differences of signal intensities that are otherwise not visible on the individual PDw, T2w and pseudo-T1 images. Within WML, these differences can be classified into subsets of bright (ADIMA-b) and dark (ADIMA-d) regions, which can be segmented using manual or semi-automated segmentation methods (see Figure 2). Henceforth, ADIMA-abnormal regions are defined as areas of hyper or hypointensity relative to the surrounding normal-appearing white matter.

Study participants

A total of 10 patients (3 males and 7 females; mean age = 53 ± 7) with clinically definite relapsing–remitting MS
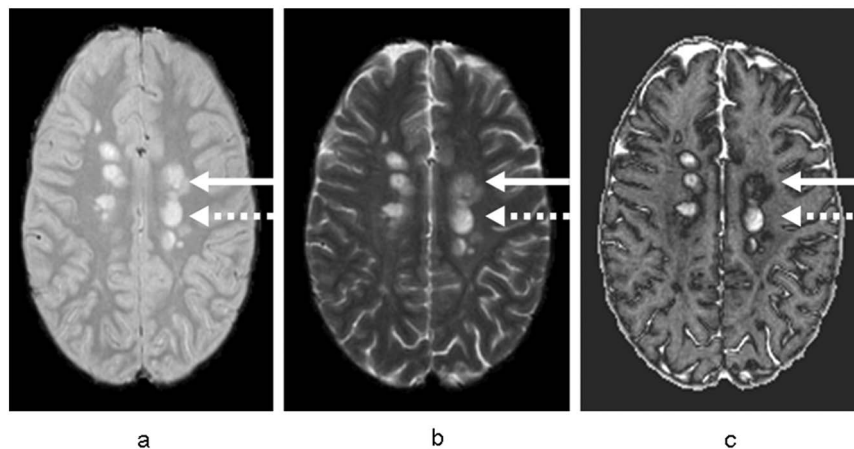
Figure 2. (a) PDw image in an MS patient with the corresponding (b) T2w image and (c) ADIMA image. The dotted white arrow shows the same hyperintense MS lesion across all image types, whereas the solid white arrow shows a hyperintense lesion on both PDw and T2w images, which has been classified into separate ADIMA-b and ADIMA-d regions.
ADIMA-b: Advanced image algebra-bright regions; ADIMA-d: Advanced image algebra-dark regions; MS: multiple sclerosis; PDw: proton density-weighted; T2w: T2-weighted

(RRMS) and an Expanded Disability Status Scale (EDSS)[13] median score of 1.5 (range 0–2.5) were recruited and then scanned, using a GE Signa 1.5T MRI system (General Electric, Milwaukee, WI, USA) and an 8-channel phased-array receive head coil. Scanning was approved by the local ethics review board and written informed consent was obtained from all study participants.

MR imaging

We acquired the following two-dimensional (2D) sequences, all with a 24 x 24 cm field of view (FOV), a matrix size of 256 x 256 and coverage of 28 x 5 mm slices:

1. Dual-echo FSE for the acquisition of PDw and T2w images with TR = 2000ms; TE1/2 = 19/95 ms; number of excitations (NEX) = 1 and echo-train length (ETL) = 8 (these images were also used to calculate T2 maps based on a two-point estimation)[14];
2. An interleaved dual-echo spin-echo sequence for MTR calculation with TR = 1720 ms; TE1/2 = 30/80 ms; both echoes with and without an MT pulse; NEX = 0.75. MTR maps were then calculated from the short echo data[15];
3. Two gradient-echo sequences used for calculating T1 maps, as previously described[16] (1st acquisition: TR = 1500 ms; TE = 11 ms; flip angle 45; NEX = 1.5 and 2nd acquisition: TR = 50 ms; TE = 11 ms; flip angle 45; NEX = 3).

Image analysis protocol

The following processing pipeline was employed:

ADIMA region masks

1. Brain extraction using BET[17] (http://www.fmrib.ox.ac.uk/fsl/); BET was initially applied to the PDw images and the resultant binary mask was also applied to the T2w images prior to the calculation of the ADIMA images.
2. ADIMA images were calculated as described above (see equations (1) and (2)), using a commercial software package (MATLAB 6, TheMathWorks Inc., Natick, MA).
3. Contours were drawn around the outer margins of the dark regions seen on the ADIMA images (i.e. ADIMA-d regions) by one rater, using a well-established semi-automated technique;[18] the original PDw and T2w images were used as a reference during the segmentation process, although dark regions seen on the ADIMA images were segmented irrespective of the appearance on the PDw and T2w images, i.e. T2-WML. This was done in order to account for the possibility that ADIMA images could depict additional (or fewer) abnormal white matter regions than usually defined by T2-WML.
4. Step 3 was repeated for the outer margin of bright regions (i.e. ADIMA-b regions) seen on the ADIMA images, to obtain the ADIMA-b mask.
5. Dark regions often surrounded bright (ADIMA-b) regions and so the ADIMA-d mask was thereafter obtained from a subtraction of the masks obtained in step 4 from step 3.
6. The sum of ADIMA-b and ADIMA-d masks (i.e. the 'combined' or ADIMA-c mask) was also obtained, for use in subsequent statistical analyses.

Conventional region masks:

1. T2-WML masks were obtained for comparison with the ADIMA-derived masks. T2-WML masks were obtained from PDw and T2w images by the same rater, using the same semi-automated technique employed for obtaining the ADIMA masks.
2. Masks were also obtained from the corresponding 2D gradient-echo T1w images (i.e. T1-WML) and pseudo-T1 images (i.e. psT1-WML) by the same rater, also using the same segmentation method.
3. NAWM regions were sampled for comparisons; two rectangular regions of a fixed size and volume (total 0.8 ml) were positioned in similar anatomical locations (within NAWM) in all 10 subjects who took part in the study.

The ADIMA-b, ADIMA-d, ADIMA-c, T2-WML, T1-WML and psT1-WML binary masks were also used to determine the percentage overlap between the various region types (i.e. to determine co-localisation).

Quantitative MR analyses

1. All quantitative scans were registered to the PDw scan using a normalised mutual information cost function,[19] so that all the images and resultant parameter maps were in the PDw and T2w (hence ADIMA) image space.
2. MTR maps were calculated from the non- and MT-weighted scans using in-house developed software based on a previously-described method.[15] ADIMA-b, ADIMA-d ADIMA-c, T2-WML, T1-WML, psT1-WML and NAWM masks were applied to the MTR maps and the mean ± standard deviation (SD) values were measured for each mask.
3. T1 parameter maps were calculated from the two gradient-echo scans as previously described[16] and regional masks were applied, as in step 2.
4. T2 parameter maps were calculated based on a two-point estimation[14] but there was no need for the registration step for the T2 maps, as these were generated from the same data-set used for calculating the ADIMA images.

Reproducibility assessment

We assessed intra-observer reproducibility of the segmentation method for the ADIMA-b regions, ADIMA-d regions and T2-WML by repeating the semi-automated segmentation process 2-times in five patients, using the same rater, with a gap of 1 month in between measurements. We assessed inter-observer reproducibility for the same region types with a second rater, who analysed the data from the same five patients, using the same semi-automated segmentation process. The second rater was blinded to the results of the first rater.

Statistical analyses

Data analysis was performed using the SPSS 11.0 statistical package (SPSS, Chicago, IL, USA) and Stata 12.1 (Stata Corporation, College Station, TX, USA). We assessed the relationships between conventional lesion volumes and the ADIMA-derived volumes using the Pearson product-moment correlation coefficients (PCC). The intra- and inter-observer coefficients of variation (COV) of the volume measurements for the ADIMA-b, ADIMA-d and conventional T2-WML, expressed as a percentage, were calculated using the mean and SD from the repeated measures using equation (3).

$$COV = 100 \times (\text{within subject SD/mean}) \qquad (3)$$

For the purpose of estimating the intra- and inter-observer agreement, the intra-class correlation coefficient (ICC) was also calculated, as the between subject variance divided by the sum of the between subject and within subject variance: This is interpretable as the proportion of variability due to biological rather than rater variation.

Repeated measures one-way analysis of variance (ANOVA) was used to compare the ADIMA-b, ADIMA-d, ADIMA-c, T2-WML, T1-WML, psT1-WML and NAWM volumes in terms of the T1, T2 and MTR quantitative measurements (i.e. a comparison of means), after checking that the variables were normally distributed. We obtained post-hoc pair-wise multiple comparisons between the groups, with p-values inflated using the Sidak adjustment[20] for multiple comparisons, and we accepted significance at $p < 0.05$. We also performed an exploratory assessment of the possible correlations between EDSS and individual lesion volumes (conventional and ADIMA-derived), using the Spearman's rank correlation.

Results

Our ADIMA images had enhanced signal heterogeneity within WML (Figure 2), but also enabled the classification of individual WML as being of either of the ADIMA-b or ADIMA-d type (Figure 3). In addition, ADIMA-b regions occasionally exhibited a hypointense rim surrounding them (i.e. classified as ADIMA-d in this case), which could not be depicted on the individual PDw or T2w images (Figure 4). Two ($n = 2$) patients out of the 10 patients investigated in this study had no ADIMA-b regions present in their images, but in those same patients we found all other region types present. All remaining patients ($n = 8$) had all the region types present in their images.

Mean volume measurements of the various region types (i.e. calculated across all patients) showed that the
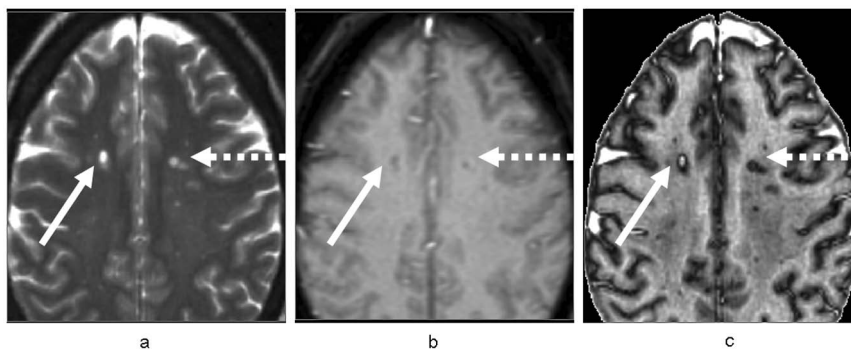
Figure 3. (a) T2w image in an MS patient with the patient's corresponding (b) T1w image and (c) ADIMA image. The solid white arrow shows a MS lesion that can be seen on both T2w and T1w images and which appeared bright on the ADIMA image, whereas the dotted white arrow shows a similar lesion that appeared dark on the ADIMA image.
ADIMA: advanced image algebra; MS: multiple sclerosis; T1w: T1-weighted; T2w: T2-weighted
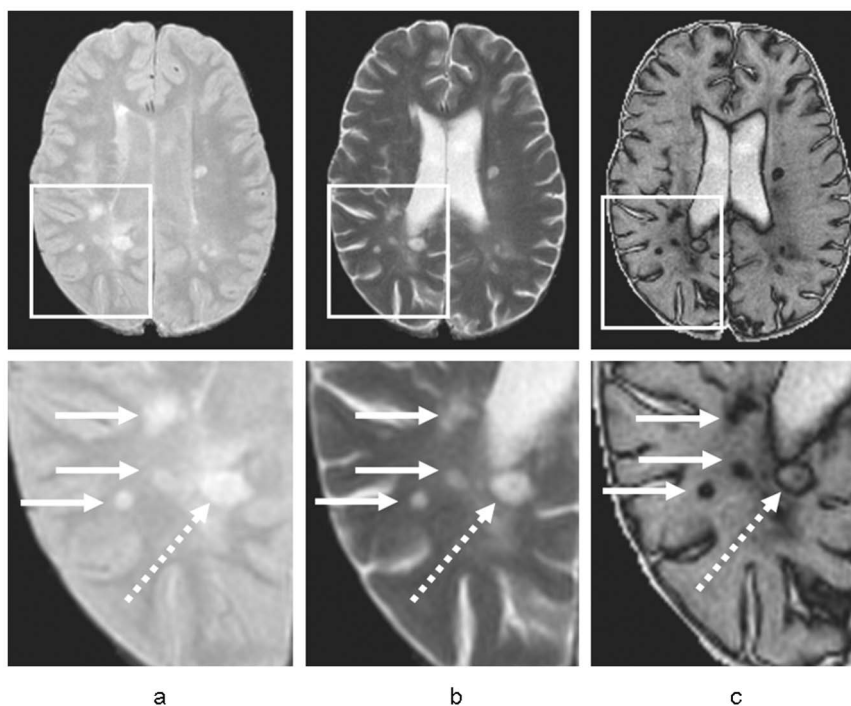

Figure 4. The top row in the figure shows (a) a PDw image with the corresponding (b) T2w image and (c) ADIMA image. The bottom row shows a magnified section of each image type, respectively. The solid white arrows show the hyperintense MS lesions on the PDw and T2w images that appeared hypointense on the ADIMA image (ADIMA-d) and the dotted white arrow shows a hyperintense lesion on the PDw and T2w images that appeared mostly hyperintense on the ADIMA image (ADIMA-b), but with a hypointense rim surrounding it (classified as being of the ADIMA-d type).
ADIMA-b: advanced image algebra, bright region; ADIMA-d: advanced image algebra, dark region; MS: multiple sclerosis; PDw: proton density-weighted; T2w: T2-weighted

ADIMA-derived volumes combined (i.e. mean ADIMA-c) exceeded the mean T2-WML volume. This meant that the ADIMA-derived regions included additional pathological regions than usually defined as T2-WML (i.e. with the semi-automated segmentation method used in this study). A breakdown of the results showed that ADIMA-b had the lowest volume, followed by the T1-WML, psT1-WML, T2-WML, ADIMA-d and ADIMA-c. Table 1 shows the mean volumes of all the region types along with significant correlations identified from pair-wise comparisons using the PCC. The mean intra-observer COV and ICC of the segmentation method used for measuring the ADIMA-b, ADIMA-d and T2-WML volumes were calculated as COV = 4.9%, 5.8%, 4.7% and ICC = 0.91, 0.92, 0.92, respectively. The mean inter-observer COV and ICC for the ADIMA-b, ADIMA-d and T2-WML were calculated as

Table 1. Mean volume measurements and pair-wise correlations between region types.[a]

Region	Volume	Pearson Correlations		
		Significant pair-wise correlations between regions	R value	P value
ADIMA-b	1.8 ml	ADIMA-b versus T2-WML	0.90	$p = 0.002$
(n = 8)		ADIMA-b versus T1-WML	0.89	$p = 0.003$
		ADIMA-b versus psT1-WML	0.88	$p = 0.004$
ADIMA-d	10.6 ml	ADIMA-d versus T2-WML	0.99	$p < 0.001$
(n = 10)		ADIMA-d versus T1-WML	0.91	$p < 0.001$
		ADIMA-d versus psT1-WML	0.81	$p = 0.004$
ADIMA-c	14.4 ml	ADIMA-c versus T2-WML	0.99	$p < 0.001$
(n = 10)		ADIMA-c versus T1-WML	0.92	$p < 0.001$
		ADIMA-c versus psT1-WML	0.81	$p = 0.014$
T2-WML	10.1 ml	T2-WML versus T1-WML	0.94	$p < 0.001$
(n = 10)		T2-WML versus psT1-WML	0.88	$p = 0.02$
T1-WML	3.3 ml	T1-WML versus psT1-WML	0.95	$p < 0.001$
(n = 10)				
psT1-WML	3.5 ml	–	–	–
(n = 10)				
NAWM	0.8 ml	–	–	–
(n = 10)				

[a]Averaged volumes for each region are given for the entire group of patients by multiplying the total number of voxels with the voxel volume.
ADIMA: Advanced image algebra; T1: T1-weighted; T2: T2-weighted; WML: white matter lesion.

Table 2. Mean % overlap between the different region types.[a]

Region Type	ADIMA-b	ADIMA-d	ADIMA-c	T2-WML	T1-WML	psT1-WML
ADIMA-b	100	–	100	90.4	67	67.2
ADIMA-d	–	100	100	60.8	16.3	14.5
ADIMA-c	18.4	81.6	100	65.5	23.3	22.1
T2-WML	20.1	65	79.3	100	33.6	28.7
T1-WML	38.9	44.5	77.6	80.2	100	46.5
psT1-WML	53.4	32.6	80.1	75.7	52	100

[a]The region types shown on the left (first column) represent the reference tissue with which comparisons can be made. For example, we saw that 90.4% of ADIMA-b contains T2-WML, whereas only 20.1% of T2-WML contains ADIMA-b.
ADIMA: advanced image algebra; T1: T1-weighted; T2: T2-weighted WML: white matter lesion

COV = 8.1%, 9.3%, 7.6% and ICC = 0.86, 0.87, 0.87, respectively.

The overlap of the various binary region masks showed that the ADIMA-b regions were almost entirely contained within T2-WML, and that they only partly overlapped with T1-WML and psT1-WML. ADIMA-d regions overlapped mainly with T2-WML, whereas the percent overlap of these regions with either the T1-WML or psT1-WML, was found to be considerably lower. T2-WML, T1-WML and psT1-WML were each found to be mostly contained within the ADIMA-c. Table 2 shows the results from all the binary region mask overlaps.

Quantitative MR measurements showed that the ADIMA-b regions had significantly higher T2 and significantly lower MTR than any of the other region types. In addition, ADIMA-b regions were found to have significantly higher T1 than any other region apart from T1-WML.

ADIMA-d regions were found to have intermediate T1, T2 and MTR values to T2-WML and NAWM; however, the differences in T1, T2 and MTR values between ADIMA-d and T2-WML were not significant, whereas the differences in each of these measures between ADIMA-d and NAWM were found to be significant. In addition, ADIMA-d regions were found to have a significant difference in T1, T2 and MTR values, when compared with either the T1-WML or psT1-WML.

ADIMA-c regions were also found to have intermediate T1, T2 and MTR values to T2-WML and NAWM. The differences in T1, T2 and MTR values between ADIMA-c and T2-WML, however, were not significant, whereas the differences in each of these measures between ADIMA-c and NAWM were found to be significant. In addition, ADIMA-c regions were found to have significant differences in T1 and MTR values, when compared with either the T1-WML

Table 3. Quantitative MRI measurements for each region type.

Measurement	ADIMA-b (*n* = 8)	ADIMA-d (*n* = 10)	ADIMA-c (*n* = 8)	T2-WML (*n* =10)	T1-WML (*n* = 10)	PseudoT1-WML (*n* = 10)	NAWM (*n* =10)
T1, mean (SD), ms	1225 (216.7)	870.1 (175.3)	917.1 (230.4)	956.2 (215.4)	1102.7 (231.6)	1076.3 (241.5)	632.8 (47.0)
T2, mean (SD), ms	213.2 (71.9)	118.5 (20.3)	130.4 (48.8)	134.2 (44.2)	156.4 (57.5)	167.2 (54.5)	79.3 (4.4)
MTR, mean (SD), %	23.8 (4.4)	32.3 (3.5)	31.4 (4.9)	30.5 (4.6)	28.1 (5.3)	27.8 (5.6)	39.7 (1.6)

ADIMA: advanced image algebra; MRI: magnetic resonance imaging; MTR: magnetisation transfer ratio; NAWM: normal-appearing white matter; T1: T1-weighted; T2: T2-weighted; WML: white matter lesion

Table 4. Statistical comparison of all the region types in terms of the quantitative measurements.[a]

Region type	Post-hoc tests	One-way ANOVA test analyses		
		p values		
		T1	T2	MTR
ADIMA-b	ADIMA-b vs. ADIMA-d	*p* < 0.001	*p* < 0.001	*p* < 0.001
	ADIMA-b vs. ADIMA-c	*p* < 0.001	*p* < 0.001	*p* < 0.001
	ADIMA-b vs. T2-WML	*p* < 0.001	*p* < 0.001	*p* < 0.001
	ADIMA-b vs. T1-WML	*p* = 0.051	*p* < 0.001	*p* < 0.001
	ADIMA-b vs. psT1-WML	*p* = 0.006	*p* = 0.02	*p* < 0.001
	ADIMA-b vs. NAWM	*p* < 0.001	*p* < 0.001	*p* < 0.001
ADIMA-d	ADIMA-d vs. ADIMA-c	*p* = 0.99	*p* = 0.99	*p* = 0.99
	ADIMA-d vs. T2-WML	*p* = 0.30	*p* = 0.99	*p* = 0.50
	ADIMA-d vs. T1-WML	*p* < 0.001	*p* = 0.05	*p* < 0.001
	ADIMA-d vs. psT1-WML	*p* < 0.001	*p* = 0.03	*p* < 0.001
	ADIMA-d vs. NAWM	*p* < 0.001	*p* = 0.04	*p* < 0.001
ADIMA-c	ADIMA-c vs. T2-WML	*p* = 0.99	*p* = 0.99	*p* = 0.99
	ADIMA-c vs. T1-WML	*p* < 0.001	*p* = 0.50	*p* = 0.008
	ADIMA-c vs. psT1-WML	*p* < 0.001	*p* = 0.08	*p* = 0.003
	ADIMA-c vs. NAWM	*p* < 0.001	*p* = 0.006	*p* < 0.001
T2-WML	T2-WML vs. T1-WML	*p* < 0.001	*p* = 0.08	*p* = 0.10
	T2-WML vs. psT1-WML	*p* = 0.02	*p* = 0.20	*p* = 0.004
	T2-WML vs. NAWM	*p* < 0.001	*p* < 0.001	*p* < 0.001
T1-WML	T1-WML vs. psT1-WML	*p* = 0.99	*p* = 0.99	*p* = 0.99
	T1-WML vs. NAWM	*p* < 0.001	*p* < 0.001	*p* < 0.001

[a]ANOVA test results for each region type with post-hoc pair-wise comparison. The *p*-values are inflated, using the Sidak adjustment for multiple comparisons, which can be used when subjects have missing values (two study patients did not have visible ADIMA-b lesions in their scans).
ADIMA: advanced image algebra; ANOVA: analysis of variance; NAWM: normal-appearing white matter; psT1: pseudo-T1; T1: T1-weighted; T2: T2-weighted; WML: white matter lesion

or the psT1-WML, but no significant differences were found in T2 values between these regions.

Table 3 shows all the results from the quantitative measurements pertaining to each region type, while Table 4 shows the results from the statistical comparison between all region types, in terms of the quantitative measurements.

The results from the exploratory assessment looking into possible correlations between lesion volumes and EDSS were not significant.

Discussion

MS WML are pathologically heterogeneous, with differing degrees of inflammation, demyelination, remyelination, axonal loss and gliosis observed.[21,22] While PDw and T2w MR images are especially sensitive in the detection of MS WML (i.e. T2-WML), they are not pathologically specific. Furthermore, the correlation between T2-WML volume and clinical disability of patients with MS is very weak, resulting in what is commonly known as a clinico-radiologic paradox.[1]

ADIMA is a novel post-processing method that utilises conventional PDw and T2w images in order to improve the dynamic range of signal intensities in these images, by means of image algebra. This study showed that in MS patients, ADIMA provides a simple and reproducible classification of WML, seen on PDw and T2w images as ADIMA-b, ADIMA-d and ADIMA-c sub-regions that can be easily segmented, with a reproducibility of segmentation comparable with other studies.[23] Importantly, this study

suggests that the sub-types of ADIMA differ in their balance of pathology, as was demonstrated by quantitative MRI, and as such they provide information that had not previously been extracted from the original PDw and T2w scans. While the ventricles and some lesions have a thin dark rim, which appears to be related to partial volume within these voxels, the ADIMA-d lesions show a higher MTR and lower relaxation times than the ADIMA-b lesions, which suggested that their fluid content is lower, indicating that the ADIMA method is detecting pathologically-related processes. Furthermore, on inspection of the ADIMA images, no systematic artefacts were observed. It is worth noting that both the blood vessels and perivascular spaces (i.e. Virchow-Robin) are visible on the ADIMA images with reversed contrast, as compared to the PDw images; however, they are no more conspicuous on the ADIMA images than on the PDw images.

By considering the results of each ADIMA-derived region individually, some interesting observations can be made. Looking at the results pertaining to the ADIMA-b regions, for example, it becomes evident that these regions are likely to represent highly destructive pathological regions in white matter that are mainly subsets of T2-WML. The high T1 and T2 values, as well as the low MTR values within these regions, suggest that the underlying tissue damage is likely to be severe and most likely is contributing to conduction impairment and deficit in a similar way to the T1-WML.[24–27] However, ADIMA-b regions are only partly contained within T1-WML. In addition, ADIMA-b regions were not present in two out of the 10 patients, while these two patients did have T1-WML. This shows that ADIMA-b and T1-WML are not entirely equivalent, which is further supported by the significant MTR and T2-relaxation time differences observed (Table 4). Perhaps the investigation of ADIMA-b regions alongside T1-WML in the future may become key in establishing any possible correlations with disability, and further studies should aim to test this hypothesis.

The ADIMA-d regions appear to have similar underlying characteristics to T2-WML. Although not significantly different, both T1 and T2 values were found to be slightly lower and the MTR slightly higher in the ADIMA-d regions than in the T2-WML. This observation can be explained by the fact that a portion of T2-WML may also include ADIMA-b (i.e. regions of much higher T1 and T2, and much lower MTR), which can influence the quantitative measurements obtained within these regions. Perhaps an important quality pertaining to ADIMA-d regions is related to the observation that these regions have highlighted additional pathological areas in white matter than T2-WML showed (i.e. with the segmentation method used in this study). This is further supported by considering the mean ADIMA-c volume, which was found to be much greater than T2-WML. A plausible explanation is related to the fact that ADIMA images are calculated using both PDw and T2w images, which means that ADIMA images are sensitive to both changes in relaxation of tissue. In vivo studies show that white matter tissue damage exists beyond the T2-WML areas, so further investigation will be required to determine what the additional pathological white matter areas that are detected on the ADIMA images truly represent.

Using the ADIMA method, we have detected lesions with a hypointense rim surrounding a bright core, something that was not seen on the PDw and T2w images. T2 hypointense rims in MS WML have been reported previously in both pathological[28] and MRI studies.[29,30] The frequency of rim lesions in a large, unselected cohort of MS patients was found to be 9%; these lesions were also found to be associated with gadolinium ring-enhancing lesions, although both lesion types could also be present independently.[29] Furthermore, the RRMS patients in the same study were found to have the highest number of these types of lesions compared to any other MS disease subtype, with neither observed in patients with the primary progressive MS (PPMS) disease subtype. This may explain why the lesions with hypointense rim were observed in this study of 10 RRMS patients, although it was not possible to determine whether the hypointensities seen on the ADIMA images represent T2 hypointense rim lesions and/or were associated with ring-enhancing lesions. Further investigations to determine the power of ADIMA to detect specific types of MS lesions will be required.

In this study, psT1-WML volumes were also measured, in order to compare these with the newly-derived ADIMA regions, as well as to determine their associations with T1-WML. By considering mean volumes between T1-WML and psT1-WML, we found these were both very similar (3.5 ml and 3.3 ml, respectively), although this finding is somewhat different from the original report showing that the mean psT1-WML area was almost half the mean T1-WML area in 17 MS patients.[12] However, in this study RRMS patients were investigated, whereas data from secondary progressive MS (SPMS) patients were analysed in the original study, so this may have influenced the results. Further studies, specifically addressing each MS disease subtype, will help us to understand the relationships between psT1-WML, T1-WML and ADIMA-derived regions.

Based on the results from the exploratory assessment looking into possible correlations between EDSS and individual lesion volumes, it was found they were not significant. This is not surprising, considering the small number of patients in this study and the extremely narrow EDSS range (0–2.5). Further investigation using larger cohorts of patients and covering a wider range of disability scores, including specific measurements like the MS functional composite MSFC measure,[31] are recommended in order to reliably determine any clinical correlations. Also, it would be interesting to assess the temporal evolution of ADIMA-b

and ADIMA-d lesions in longitudinal studies of patients with MS, to assess any potential for prediction of disease progression.

In summary, ADIMA is presented as a new post-processing method that enables a simple classification of WML into two groups, with different quantitative MR properties, that can be reproducibly segmented. Future work to understand the nature of the ADIMA-derived regions in MS could include post-mortem investigations with matching histopathologic correlates. Furthermore, investigations of the behaviour of the ADIMA method at higher magnetic field strengths may also be useful in further defining the method in vivo. A larger clinical study that includes all MS clinical subgroups is warranted as well, to understand clinical correlations with the new ADIMA-derived regions. Studies of other white matter diseases could help assess whether the ADIMA method might someday be helpful in providing a differential diagnosis. A facilitating characteristic of the ADIMA method in this respect, is that it can actually be applied retrospectively, to already available MR data-sets.

Funding

Conflict of interest

The authors declare that there are no conflicts of interest.

References

1. Barkhof F. The clinico-radiological paradox in multiple sclerosis revisited. *Curr Opin Neurol* 2002; 15: 239–245.

2. Filippi M, Campi A, Dousset V, et al. A magnetization transfer imaging study of normal-appearing white matter in multiple sclerosis. *Neurology* 1995; 45: 478–482.

3. Loevner LA, Grossman RI, Cohen JA, et al. Microscopic disease in normal-appearing white matter on conventional MR images in patients with multiple sclerosis: Assessment with magnetization transfer measurements. *Radiology* 1995; 196: 511–515.

4. Ciccarelli O, Werring DJ, Wheeler-Kingshott CA, et al. Investigation of MS normal-appearing brain using diffusion tensor MRI with clinical correlations. *Neurology* 2001; 56: 926–933.

5. Laule C, Vavasour IM, Moore GR, et al. Water content and myelin water fraction in multiple sclerosis. A T2 relaxation study. *J Neurol* 2004; 251: 284–293.

6. Fernando KT, McLean MA, Chard DT, et al. Elevated white matter myo-inositol in clinically isolated syndromes suggestive of multiple sclerosis. *Brain* 2004; 127: 1361–1369.

7. Inglese M, Li BS, Rusinek H, et al. Diffusely elevated cerebral choline and creatine in relapsing–remitting multiple sclerosis. *Magn Reson Med* 2003; 50: 190–195.

8. Ge Y, Grossman RI, Babb JS, et al. Dirty-appearing white matter in multiple sclerosis: Volumetric MR imaging and magnetization transfer ratio histogram analysis. *Am J Neuroradiol* 2003; 24: 1935–1940.

9. Vrenken H, Seewann A, Knol DL, et al. Diffusely abnormal white matter in progressive multiple sclerosis: In vivo quantitative MR imaging characterisation and comparison between disease types. *Am J Neuroradiol* 2010; 31: 541–548.

10. Seewann A, Vrenken H, Van der Valk P, et al. Diffusely abnormal white matter in chronic multiple sclerosis: Imaging and histopathologic analysis. *Arch Neurol* 2009; 66: 601–609.

11. Moore GR, Laule C, MacKay A, et al. Dirty-appearing white matter in multiple sclerosis: Preliminary observations of myelin phospholipid and axonal loss. *J Neurol* 2008; 255: 1802–1811.

12. Hickman SJ, Barker GJ, Molyneux PD, et al. Technical note: The comparison of hypointense lesions from 'pseudo-T1' and T1-weighted images in secondary progressive multiple sclerosis. *Mult Scler* 2002; 8: 433–443.

13. Kurtzke JF. Rating neurologic impairment in multiple sclerosis: An Expanded Disability Status Scale (EDSS). *Neurology* 1983; 33: 1444–1452.

14. Duncan JS, Bartlett P and Barker GJ. Technique for measuring hippocampal T2 relaxation time. *Am J Neuroradiol* 1996; 17: 1805–1810.

15. Barker GJ, Tofts PS and Gass A. An interleaved sequence for accurate and reproducible clinical measurement of magnetization transfer ratio. *Magn Reson Imaging* 1996; 14: 403–411.

16. Parker GJM, Barker GJ and Tofts PS. Accurate multislice gradient echo T1 measurement in the presence of non-ideal rf pulse shape and RF field nonuniformity. *Magn Reson Med* 2001; 45: 838–845.

17. Smith SM. Fast robust automated brain extraction. *Human Brain Mapping* 2002; 17: 143–155.

18. Molyneux PD, Tofts PS, Fletcher A, et al. Precision and reliability for measurement of change in MRI lesion volume in multiple sclerosis: A comparison of two computer assisted techniques. *J Neurol Neurosurg Psychiatry* 1998; 65: 42–47.

19. Studholme C, Hill DLG and Hawkes DJ. An overlap invariant entropy measure of 3D medical image alignment. *Pattern Recog* 1999; 32: 71–86.

20. Šidàk Z. Rectangular confidence region for the means of multivariate normal distributions. *J Am Statistical Ass* 1967; 62: 626–633.

21. Ferguson B, Matyszak MK, Esiri MM, et al. Axonal damage in acute multiple sclerosis lesions. *Brain* 1997; 120: 393–399.

22. Trapp BD, Peterson J, Ransohoff RM, et al. Axonal transection in the lesions of multiple sclerosis. *NEJM* 1998; 338: 278–285.

23. Filippi M, Horsfield MA, Rovaris M, et al. Intraobserver and interobserver variability in schemes for estimating the volume of brain lesions on MR images in multiple sclerosis. *Am J Neuroradiol* 1998; 19: 239–244.

24. Bruck W, Bitsch A, Kolenda H, et al. Inflammatory central nervous system demyelination: Correlation of magnetic resonance imaging findings with lesion pathology. *Ann Neurol* 1997; 42: 783–793.

25. Van Walderveen MA, Kamphorst W, Scheltens P, et al. Histopathologic correlate of hypointense lesions on T1-weighted spin-echo MRI in multiple sclerosis. *Neurol* 1998; 50: 1282–1288.

26. Van Waesberghe JH, Kamphorst W, De Groot CJ, et al. Axonal loss in multiple sclerosis lesions: Magnetic resonance imaging insights into substrates of disability. *Ann Neurol* 1999; 46: 747–754.

27. Schmierer K, Tozer DJ, Scaravilli F, et al. Quantitative magnetization transfer imaging in post-mortem multiple sclerosis brain. *J Magn Reson Imaging* 2007; 26: 41–51.

28. Lucchinetti CF, Gavrilova RH, Metz I, et al. Clinical and radiographic spectrum of pathologically confirmed tumefactive multiple sclerosis. *Brain* 2008; 131: 1759–1775.

29. Llufriu S, Pujol T, Blanco Y, et al. T2 hypointense rims and ring-enhancing lesions in MS. *Mult Scler* 2010; 16: 1317–1325.

30. Haacke EM, Makki M, Ge Y, et al. Characterizing iron deposition in multiple sclerosis lesions using susceptibility weighted imaging. *J Magn Reson Imaging* 2009; 29: 537–544.

31. Fischer JS, Rudick RA, Cutter GR, et al. The Multiple Sclerosis Functional Composite Measure (MSFC): An integrated approach to MS clinical outcome assessment. *Mult Scler* 1999; 5: 244–250.